J Neurophysiol 115: 2830–2839, 2016.
First published March 16, 2016; doi:10.1152/jn.00097.2016.

Muscle fatigue increases beta-band coherence between the firing times of simultaneously active motor units in the first dorsal interosseous muscle

Lara McManus,[1] Xiaogang Hu,[2] William Z. Rymer,[3,4] Nina L. Suresh,[3] and Madeleine M. Lowery[1]
[1]*University College Dublin, Belfield, Dublin, Ireland;* [2]*Joint Department of Biomedical Engineering, University of North Carolina-Chapel Hill and North Carolina State University, Chapel Hill, North Carolina;* [3]*Rehabilitation Institute of Chicago, Chicago, Illinois; and* [4]*Northwestern University, Evanston, Illinois*

Submitted 3 February 2016; accepted in final form 15 March 2016

McManus L, Hu X, Rymer WZ, Suresh NL, Lowery MM. Muscle fatigue increases beta-band coherence between the firing times of simultaneously active motor units in the first dorsal interosseous muscle. *J Neurophysiol* 115: 2830–2839, 2016. First published March 16, 2016; doi:10.1152/jn.00097.2016.—Synchronization between the firing times of simultaneously active motor units (MUs) is generally assumed to increase during fatiguing contractions. To date, however, estimates of MU synchronization have relied on indirect measures, derived from surface electromyographic (EMG) interference signals. This study used intramuscular coherence to investigate the correlation between MU discharges in the first dorsal interosseous muscle during and immediately following a submaximal fatiguing contraction, and after rest. Coherence between composite MU spike trains, derived from decomposed surface EMG, were examined in the delta (1–4 Hz), alpha (8–12 Hz), beta (15–30 Hz), and gamma (30–60 Hz) frequency band ranges. A significant increase in MU coherence was observed in the delta, alpha, and beta frequency bands postfatigue. In addition, wavelet coherence revealed a tendency for delta-, alpha-, and beta-band coherence to increase during the fatiguing contraction, with subjects exhibiting low initial coherence values displaying the greatest relative increase. This was accompanied by an increase in MU short-term synchronization and a decline in mean firing rate of the majority of MUs detected during the sustained contraction. A model of the motoneuron pool and surface EMG was used to investigate factors influencing the coherence estimate. Simulation results indicated that changes in motoneuron inhibition and firing rates alone could not directly account for increased beta-band coherence postfatigue. The observed increase is, therefore, more likely to arise from an increase in the strength of correlated inputs to MUs as the muscle fatigues.

motor unit coherence; isometric fatigue; intramuscular coherence; beta-band coherence; short-term synchronization

AS MUSCLE FATIGUE PROGRESSES, a number of adaptations develop within the central and peripheral nervous system, several of which may serve as compensatory or protective mechanisms. These include alterations in motor unit (MU) recruitment and firing rate (McManus et al. 2015a), changes in reflex inputs from metabolically and mechanically sensitive muscle afferents (Macefield et al. 1991), and a progressive reduction in the ability to voluntarily activate the muscle with suboptimal drive from the motor cortex (Gandevia 2001). In addition to these more well-established changes, it is commonly suggested that fatigue also alters the degree of synchronization between the firing times of simultaneously active MUs. Recent studies have added weight to this hypothesis, reporting evidence of a fatigue-induced increase in synchronized MU firings using indirect estimates of synchronization derived from surface electromyographic (EMG) interference signals (Beretta-Piccoli et al. 2015; Holtermann et al. 2009; Talebinejad et al. 2010; Webber et al. 1995). The observed synchronization of MU firing trains can be modulated in specific frequency ranges, including the delta (1–4 Hz), alpha (8–12 Hz), beta (15–30 Hz), and gamma (30–60 Hz) frequency bands. Each type of synchrony is purported to have distinct origins, with beta-band coherence being of particular interest because it is believed to reflect information on oscillatory cortical and subcortical processes and has been shown to be directly correlated with short-term MU synchronization (Lowery et al. 2007). Despite indications of increased MU synchronization postfatigue, direct evidence of an increase in either short-term synchronization or coherent MU firings in the beta frequency range has never been shown.

Previous studies using intramuscular EMG have reported no change in MU synchronization with fatigue (Contessa et al. 2009; Nordstrom et al. 1990), with the exception of an early study that reported increased MU synchrony following a sustained, fatiguing maximal contraction in the biceps (Buchthal and Madsen 1950). However, in that study MUs were recorded after the recovery of muscle force, which makes it unclear whether the increase in MU synchronization was due to fatigue or could be attributed to exercise-induced muscle damage (Dartnall et al. 2008). The conflicting results obtained from intramuscular EMG studies may arise from the relatively low number of MUs detected. This could also explain why methods based on nonlinear analysis of the surface EMG signal, which captures a larger representative sample of MU activity, have consistently inferred that MU synchronization increases with fatigue (Beretta-Piccoli et al. 2015; Holtermann et al. 2009; Talebinejad et al. 2010; Webber et al. 1995). Analysis of a greater number of MU spike trains using surface EMG decomposition techniques has the potential to enhance the detection of correlated MU discharges.

Several recent studies have shown a fatigue-induced increase in intermuscular beta coherence between surface EMG of synergistic index finger flexor muscles (Kattla and Lowery 2010), knee extensor muscles (Chang et al. 2012), and antagonistic elbow muscles (Wang et al. 2015) and during three-digit grasping (Danna-Dos Santos et al. 2010). Furthermore, increased beta-band coherence was observed between cortical neuron activity and EMG recordings following sustained maximal (Tecchio et al. 2006) and submaximal fatiguing contractions (Ushiyama et al. 2011). Although increases in beta frequency corticomuscular and intermuscular coherence post-

Address for reprint requests and other correspondence: L. McManus, Univ. College Dublin, Belfield, Dublin 4, Ireland (e-mail: lara.mc-manus@ucdconnect.ie).

0022-3077/16 Copyright © 2016 the American Physiological Society

Downloaded from www.physiology.org/journal/jn at Univ Col Dublin (137.043.113.222) on April 1, 2019.

fatigue have been reported, direct evidence of a similar change in coherent MU discharges within the same muscle has not been shown. The aim of this study was to examine alterations in MU coherence during and after a sustained submaximal fatiguing contraction in the first dorsal interosseous. To do this, a large population of MU spike trains, decomposed from the surface EMG signal, were examined. Coherence between groups of simultaneously active MUs was then calculated across a range of frequency bands before, during, and directly after the fatiguing contraction and again following a rest period. In addition, the temporal evolution of synchronized MU firing was investigated over the course of the fatiguing contraction using wavelet coherence. Finally, model simulations were used to explore whether changes in mean MU firing rates or alterations in the direct inhibition of motoneurons could account for the changes in coherence observed.

Direct evidence of an increase in short-term MU synchronization and correlated MU firings in the beta-band range during fatigue within a single muscle is been presented for the first time in this study. An increase in delta-band coherence, which is equivalent to the "common drive" modulation of MU firing rates (Myers et al. 2004), and alpha-band coherence were also reported both during the sustained contraction and postfatigue. The increase in delta-band coherence was correlated with increases in force variability. A progressive decrease in MU mean firing rates (MFR) was observed during the fatiguing contraction; however, model simulations indicated that changes in firing rates alone were unlikely to account for the increase in coherence postfatigue. Preliminary results from this study were presented at the 7th Annual International IEEE EMBS Conference on Neural Engineering (McManus et al. 2015b).

METHODS

Experimental procedure. Written informed consent and ethical approval was obtained for 15 subjects (8 female) to examine EMG activity of the first dorsal interosseous muscle during isometric abduction of the right index finger. Details of the experimental procedure have been reported previously in McManus et al. (2015a). Briefly, subjects performed a series of six isometric voluntary contractions prefatigue. The force trajectory contained a 3-s quiescent period for baseline noise calculation, an up-ramp increasing at 10% maximum voluntary contraction (MVC) per second, a constant force of 20% MVC for 10 s, a down-ramp decreasing at 10% MVC/s, and a final 3-s quiescent period. After the six prefatigue trials, a sustained isometric contraction was performed at 30% MVC until task failure, defined as the point at which the subject's force dropped 10% below the required output for 5 s or longer. Additional verbal encouragement was provided during the contraction. A single MVC was performed directly following task failure, followed by six 10-s contractions at 20% MVC with no rest period between trials to minimize recovery. Subjects were then allowed a 10-min recovery period before performing a series of four more 10-s contractions at 20% MVC.

Data analysis: MU acceptance. Discriminable MUs were extracted from the surface EMG recorded using the decomposition algorithms described in Nawab et al. (2010) (Delsys, version 4.1.1.0). For each identified MU, the output of the algorithm consisted of MU firing times and four motor unit action potential (MUAP) waveforms corresponding to four pairs of electrode channels. The identified firing times for each MU were used to spike trigger average (STA) the surface EMG signal on each channel, resulting in four representative STA MUAP estimates for each MU. Two separate reliability tests were performed to determine which decomposed MUs would be retained for further analysis, using the procedure outlined in Hu et al. (2013). To quantify the variation of the STA MUAP over time, the coefficient of variation was calculated for the peak-to-peak amplitude of the MUAP templates. The maximum linear correlation coefficient between the STA estimate (calculated over the entire trial duration) and the decomposition-estimated template was also computed. MUs with an average correlation coefficient (between the STA MUAP estimate and the decomposition MUAP template) >0.7 and a coefficient of variation of the peak-to-peak amplitude <0.3 across all four channels were selected for further analysis.

In the present study, the MUs identified by the decomposition algorithm during the fatiguing contraction were additionally required to have a correlation coefficient (between the STA MUAP template and the decomposition MU template and between each consecutive STA MUAP template and the average STA MUAP template) >0.8 and a peak-to-peak MUAP amplitude variation <0.2 (both between consecutive STA MUAP templates and across all STA MUAP templates) on a minimum of two channels to be selected for further analysis. A 400-ms Hanning window filter was applied to the firing time data to analyze trends in MU mean firing times over the course of the fatiguing contraction. The change in firing rate was examined for each MU by fitting a least-squares regression line to the MFR data.

Data analysis: MU coherence, wavelet coherence, and short-term synchronization. The number of MU spike trains used for the coherence analysis was chosen to be the maximum number of MU spike trains available across all accepted trials and conditions for each subject. This ensured that an equal sample of MU spike trains was analyzed within each condition. For trials that contained more than the chosen number of MUs for that subject, MU spike trains were selected randomly for further analysis. The spike trains from multiple trials were pooled together for each condition, with the same number of trials analyzed per condition. The pooled MU trains were then divided into two groups, and the firing instances in each group were summed to obtain two composite spike trains (Fig. 1). The composite spike train method has been previously applied to examine corticomuscular coherence and low-frequency (<10 Hz) intramuscular coherence during fatigue among a small number of subjects (Castronovo et al.

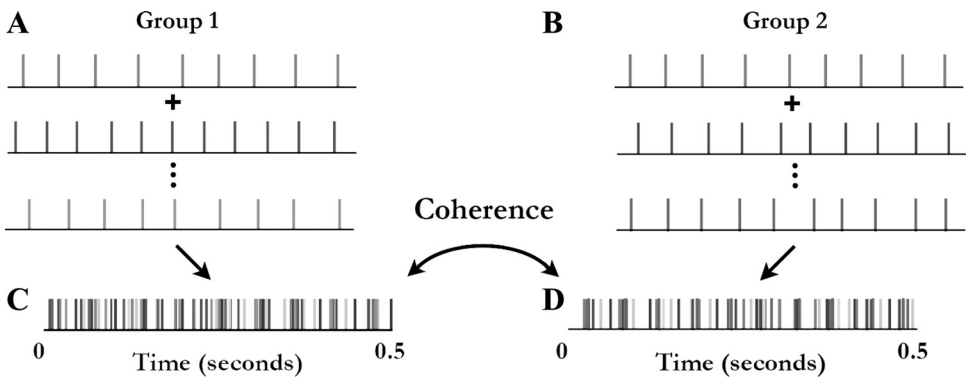

Fig. 1. Two sample groups of MU spike trains (*A* and *B*) pooled to form composite MU spike trains (*C* and *D*). The coherence between the 2 composite firing trains in *C* and *D* was then estimated.

Downloaded from www.physiology.org/journal/jn at Univ Col Dublin (137.043.113.222) on April 1, 2019.

2015). A pair of composite spike trains was obtained for every available combination of two groups from the pooled MUs. For each subject, the number of paired combinations of composite trains analyzed was constant across prefatigue, postfatigue, and recovery conditions.

The magnitude squared coherence, $C_{xy}(f)$, was calculated for each pair of composite spike trains, $x(t)$ and $y(t)$, as a function of their power spectral densities, $P_{xx}(f)$ and $P_{yy}(f)$, and cross power spectral density, $P_{xy}(f)$:

$$C_{xy}(f) = \frac{|P_{xy}(f)|^2}{P_{xx}(f)P_{yy}(f)}, \quad (1)$$

The level at which the magnitude squared coherence was considered significant for overlapping windows with 75% overlap was calculated at the 0.05 significance level (Terry and Griffin 2008). The coherence in each frequency band was estimated as the integral of the magnitude-squared coherence above the significance level, for the delta (1–4 Hz), alpha (8–12 Hz), beta (15–30 Hz), and gamma (30–60 Hz) frequency bands. The coherence was estimated for three conditions: prefatigue, postfatigue, and following the recovery period.

Coherence was estimated for each combination of composite MU trains. The prefatigue coherence estimates were standardized to have zero mean and unit variance (see Fig. 4). Postfatigue and recovery coherence estimates were then scaled using the prefatigue mean and variance for that subject. Fourier-based coherence was used for the short-duration contractions pre- and postfatigue, which were assumed to be stationary.

For the longer, nonstationary fatiguing contractions, wavelet coherence analysis was used to examine the temporal evolution of the intramuscular coherence (Lachaux et al. 2002). The wavelet transform, $W_x(b, s)$, of a signal $x(u)$ is given by the convolution of the signal with a wavelet function, where b and s are the time shift and scale, respectively. For this study, the Morlet waveform $\Psi_{s,b}(u)$ was chosen because it has both oscillatory features and is complex valued. Similar to Fourier-based coherence, the wavelet coherence $W\mathrm{Co}(t, f)$ at a time t and frequency f between two signals $x(t)$ and $y(t)$ is defined by

$$WCo(t, f) = \frac{|SW_{xy}(t, f)|}{[SW_{xx}(t, f) \cdot SW_{yy}(t, f)]^{1/2}}, \quad (2)$$

where $SW_{xy}(t, f)$ is the wavelet cross-spectrum between $x(t)$ and $y(t)$ and $SW_{xx}(t, f)$ and $SW_{yy}(t, f)$ are the autospectra of the two signals. In the wavelet coherence method, the length of the integration window decreases with increasing frequency, which improves the temporal resolution of the coherence estimate for higher frequencies. The number of cycles of the wavelet ($n_{co} = 10$) and the number of cycles contained within the integration window ($n_{cy} = 40$) were chosen to focus on the change in beta-band wavelet coherence. Confidence levels for the detection of significant coherence were calculated for these values of n_{co} and n_{cy} by using surrogate white noise signals to compute the statistical thresholds (Lachaux et al. 2002). Wavelet coherence was used to examine the coherence between composite MU spike trains over the fatiguing contraction. Each subject was required to have a minimum number of eight MUs to pass the acceptance criteria to be used in the wavelet coherence analysis. For subjects with a large number of MUs, 100 combinations were randomly chosen for the coherence estimate.

For each subject, the integral of the coherence in the alpha, beta, and gamma frequency bands was calculated at each 1-ms time step over the course of the fatiguing contraction. The change in coherence during the fatiguing contraction was examined for each subject by fitting a least-squares regression line to the integral of the coherence in each frequency band against the percentage of time to task failure and using the equation of the line to calculate the estimates for the initial and final coherence values. The percentage change in coherence in each frequency band was compared with the percent change in the coefficient of variation of the force trace, calculated during the first and the last 10 s of the fatiguing contraction.

In the time domain, short-term MU synchronization was quantified using the synchronization index (SI; De Luca et al. 1993). Cross-interval histograms were constructed between pulse trains representing the firing times of pairs of MUs for each possible pair of MUs. The cross-interval histogram was constructed by calculating the first-order, forward, and backward recurrence times of the alternate MU with respect to the reference unit. The peak in the cross-interval histogram was determined by locating bins within 6 ms of the zero time lag, for which the total number of occurrences lay above the mean number of occurrences at the 95% significance level. SI, the percentage of synchronized firings in excess of what would be expected due to chance, was defined as the ratio between the total number of firings within the peak in excess of the mean and half the total area under the cross-interval histogram. The synchronization between MU pairs was calculated for the first and second half of each fatiguing contraction.

Model simulation. A model of the motoneuron pool, surface EMG signal, and force output of first dorsal interosseous muscle was used to examine the degree to which synchronization and coherence between the MU discharge times is affected by the strength of common presynaptic inputs to the motoneuron pool, as well as possible additional factors including variations in mean MU firing rate and the introduction of a common inhibitory input.

The model was designed to produce MU activation patterns qualitatively similar to those recorded experimentally. The force generated by the model was continuously compared with a target force and adjusted on the basis of the difference between the two to emulate the experimental conditions in which a subject tracks a target force trajectory. The model of the motoneuron pool was based on the model described by Lowery and Erim (2005) and comprised 100 motoneurons, simulated using a single-compartment threshold-crossing model (Powers 1993). Each motoneuron received three inputs: a constant activation current, a common modulation or oscillatory current, and an independent membrane noise voltage (Lowery and Erim 2005).

The motoneuron pool model was coupled to a model of the surface EMG signal based on that described in Lowery et al. (2000) and adapted for the first dorsal interosseous muscle. The muscle was assumed to be trapezoidal in shape with a width of 35 mm, height of 5 mm, and length of 11.5 mm on the medial side extending to 35 mm on the lateral side (Infantolino and Challis 2010). Coordinates within the muscle cross section for both MUs and fibers within each MU were randomly generated for 100 MUs using Sobol distributions. The number of fibers assigned to each MU was assumed to increase linearly with recruitment threshold from 50 to 360 (Feinstein et al. 1955). Fiber diameters (0.052–0.068 mm; Freund 1983) also increased linearly with MU size, and a muscle fiber density of 20 fibers/mm^2 was assumed (Buchthal et al. 1957). All muscle fibers were orientated with a pennation angle of 50° (Infantolino and Challis 2010). The electrode was modeled as 5-point electrodes located at each of the corners and the center of a 5 × 5-mm square, based on the dimensions of the Delsys electrode used experimentally. It was located 15 mm from the proximal end of the muscle and 11 mm from the lateral side of the muscle, 3.5 mm above most superficial muscle fibers, and rotated 20° with respect to the fiber direction to replicate experimental placement of the electrode. The muscle fibers were located within homogeneous cylindrically anisotropic muscle tissue, with radial and axial conductivities of 0.063 and 0.33 S/m, respectively. The single fiber action potential detected when each muscle fiber was stimulated was calculated using an infinite volume conductor model for anisotropic muscle (Lowery et al. 2000). The single fiber action potentials generated by all of the fibers in each MU were summed linearly to yield the MUAP. The common input was simulated by bandpass filtering a random Gaussian signal between 9 and 25 Hz using a second-order Butterworth filter, chosen to generate MU coherence spectra qualitatively similar to those recorded experimentally. The amplitude of the signal was varied between 0 and 0.6 mV

Downloaded from www.physiology.org/journal/jn at Univ Col Dublin (137.043.113.222) on April 1, 2019.

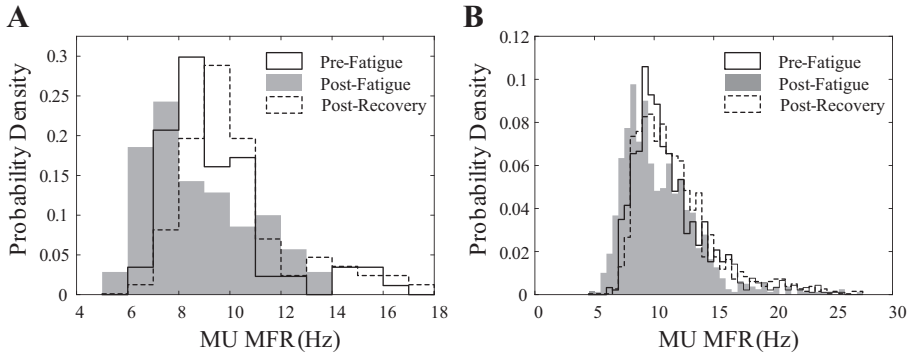

Fig. 2. Probability density of MU MFR for a single representative subject (*A*) and across all subjects (*B*).

to simulate changing levels of shared presynaptic input in the beta band.

To investigate whether a net inhibition of motoneurons could affect the level of MU coherence, inhibition to the motoneuron pool was simulated as follows. Firing of a motoneuron resulted in the generation of an inhibitory postsynaptic potential (IPSP) at the input to that motoneuron and to its two neighboring motoneurons as defined in terms of the motoneuron recruitment order. To replicate the changes in firing rate and recruitment that were observed experimentally, a weighting function was assigned to the amplitude of the IPSPs such that the earliest recruited motoneurons received the greatest level of inhibition. IPSPs were simulated as an alpha function with a rise time of 5.5 ms and half-width of 18.5 ms, and ranged in amplitude from 5 to 60 μV according to a weighted sigmoidal function, based on experimental data of Renshaw inhibition (Hamm et al. 1987).

STA was performed on the simulated EMG data to characterize the MU waveform, using the same acceptance criteria as in the experimental data. To estimate MU coherence from the motoneuron model, 26 MUs were randomly chosen from the pool and coherence was estimated for the composite spike trains for the first 10,000 combinations of two groups, as described previously for the experimental data.

Statistical analysis. A repeated-measures analysis of variance was conducted to compare MU MFR and coherence in each frequency band prefatigue, postfatigue, and following the recovery period. Mauchly's test of sphericity was implemented to check the assumption of sphericity, and if violated, a Greenhouse-Geisser correction was applied. Post hoc tests to examine pairwise differences between conditions were conducted using the Fisher's least significant difference test.

The relationship between initial MU firing rate (the intercept of the regression line) and the change in the MU firing rate over the course of the fatiguing contraction (slope of the line) was examined using a Pearson product-moment correlation. The *t*-statistic was used to test for the significance of the slope. The relationship between the change in MU MFR and the change in beta-band coherence was investigated using a Spearman's rank-order nonparametric correlation. A Spearman's correlation was also used to assess the relationship between the initial coherence and the percent change in coherence over the course of the fatiguing contraction in the delta, alpha, beta, and gamma bands and the correlation between the percent change in coherence and the percent change in the coefficient of variation of the force. Differences in the median SI between the first and second half of the fatiguing contraction were tested using a paired Wilcoxon signed-rank test.

RESULTS

Maximum voluntary force was significantly reduced (from 50.4 ± 11 to 26 ± 12 N, $P < 0.001$) following the sustained isometric fatiguing contraction (248 ± 174 s). MVC failed to recover after the period of rest and remained significantly depressed (39.5 ± 15.9 N, $P < 0.001$), though still higher than directly postfatigue ($P < 0.005$). The average number of MUs detected per trial was 17.6 ± 3 prefatigue, 15.5 ± 3.5 postfatigue, and 17.2 ± 3.8 after recovery, with 80 ± 10% of MUs accepted for further analysis. During the fatiguing contraction, 11 of 15 subjects had the minimum of 8 accepted MUs required to be included in the wavelet coherence analysis. For these subjects, an average of 70 ± 11 MUs were identified by the decomposition algorithm, but due to more stringent criteria applied to the sustained fatiguing contraction, just 27.7 ± 14% of these MUs were accepted.

Motor unit properties pre- and postfatigue. A small but significant effect of fatigue on the MFR of the decomposed MUAPs was observed [$F(2, 22) = 10.04$, $P < 0.001$; Fig. 2*B*]. MU MFR decreased significantly ($P < 0.005$) from pre- to postfatigue conditions (10.8 ± 1.2 vs. 10.0 ± 1.4 Hz, respectively). After the recovery period, MU firing rates increased (11.2 ± 1.2 Hz, $P < 0.001$) and were not statistically different from discharge rates observed before fatigue ($P = 0.15$).

The coherence between composite MU pulse trains is displayed in Fig. 3 prefatigue, postfatigue, and after recovery for a representative subject. A significant increase in MU coherence was observed in the delta (0.64 ± 0.98 to 4.14 ± 2.4, $P < 0.0001$), alpha (6.2 ± 3.6 to 10.8 ± 5, $P < 0.0001$), and beta (13.9 ± 7.3 to 25.6 ± 10.2, $P < 0.0001$) frequency bands postfatigue. The means and SD of the standardized coherence values across all MU combinations are presented in Fig. 4 for the delta (*A*), alpha (*B*), beta (*C*), and gamma (*D*) frequency bands.

Following the recovery period, coherence decreased significantly and was not significantly different from the estimated coherence prefatigue for the delta, alpha, and beta frequency bands ($P = 0.3$, $P = 0.9$, and $P = 0.42$, respectively). The changes in gamma frequency coherence did not exhibit a

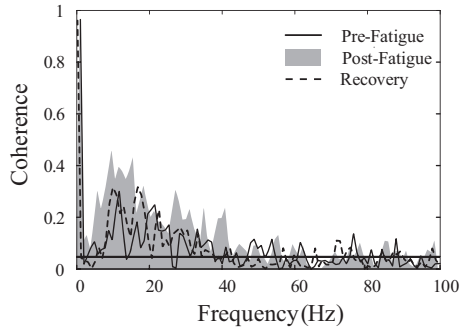

Fig. 3. Highest coherence between composite MU spike trains observed across MU combinations prefatigue, postfatigue, and following a recovery period for a representative subject (with a 95% confidence interval).

Downloaded from www.physiology.org/journal/jn at Univ Col Dublin (137.043.113.222) on April 1, 2019.

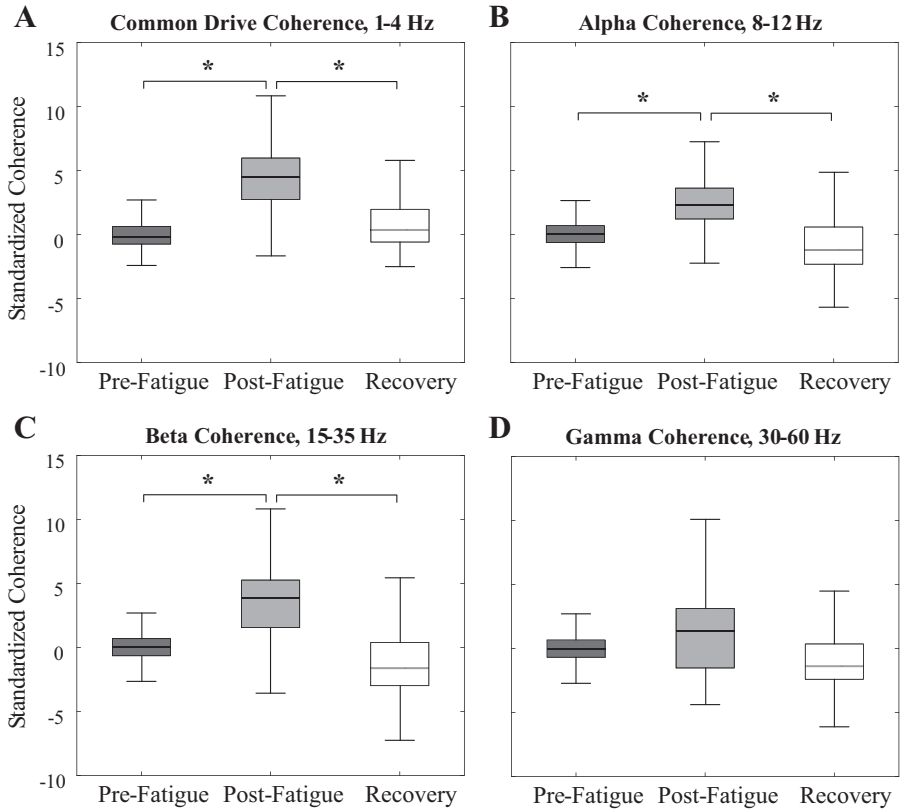

Fig. 4. Median and SD of the standardized coherence values across all MU combinations for the common drive (1–4 Hz; *A*), alpha (8–12 Hz; *B*), beta (15–30 Hz; *C*), and gamma (30–60 Hz; *D*) frequency bands. $*P < 0.001$.

statistically significant effect of condition [$F(1.29, 18) = 3.1$, $P = 0.087$; Fig. 4*D*].

Fatiguing contraction: motor unit mean firing rate. To investigate the MU MFR changes in more detail, MU MFR were analyzed for 11 subjects over the course of the fatiguing contraction, with an average of 16.9 ± 6.7 MUs per subject and an initial MFR of 12.8 ± 2.8 Hz. Across all subjects, there was a weak tendency for MUs with higher firing rates to exhibit a decrease in discharge rate during the fatiguing contraction and for those with lower firing rates to increase their MFR ($r = -0.27$, $P < 0.001$). For 6 of the 11 subjects there was a significant, strong negative correlation between initial MU firing rate and the change in the MU firing rate over the course of the contraction ($r = -0.7 \pm 0.09$; Fig. 5*A*). Over all subjects, a weak correlation between the two variables was still present ($r = -0.27$, $P < 0.001$; Fig. 5*B*). The majority of MUs (74.4%) exhibited a decline in MFR over the course of the fatiguing contraction, although the average magnitude of the decline was small, −10 ± 9.4%, and there was a large variation in the magnitude of MU MFR changes per subject. In the remaining MUs, the MFR increased by an average of 14.7 ± 27.5%. MUs recruited as the contraction progressed exhibited both increases and decreases in their discharge rates.

Fatiguing contraction: motor unit coherence and synchronization. Wavelet coherence and time-domain synchronization between MU firing times were analyzed for the same 11 subjects during the fatiguing contraction. The majority of subjects exhibited an increase in coherence in the delta, alpha, and beta band over the course of the fatiguing contraction, with median regression slopes of 0.004 ± 0.006, 0.012 ± 0.01, and 0.014 ± 0.03, respectively. MU firing rates and the corresponding MU wavelet coherence during the fatiguing contraction are shown for a representative subject in Fig. 6, *A* and *B*. In the gamma frequency band, only five subjects showed an increase in coherence, with positive regression slopes significantly different from zero. There was a significant negative correlation between the initial value for delta-, alpha-, and beta-band coherence and the percent change in coherence

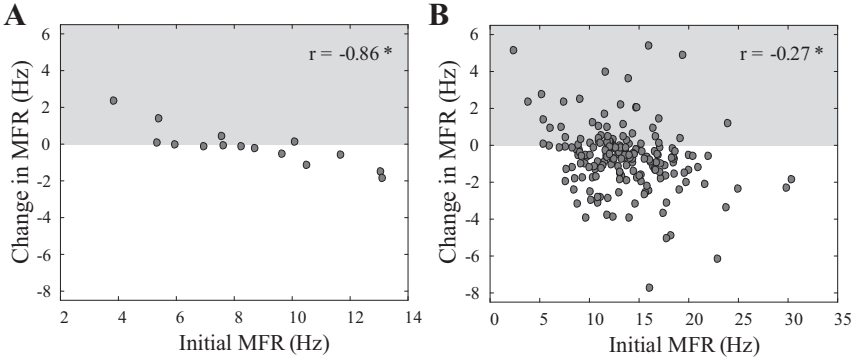

Fig. 5. Change in MFR for each MU during the fatiguing contraction as a function of that unit's initial firing rate for a single subject (*A*) and across all subjects (*B*). $*P < 0.001$.

Downloaded from www.physiology.org/journal/jn at Univ Col Dublin (137.043.113.222) on April 1, 2019.

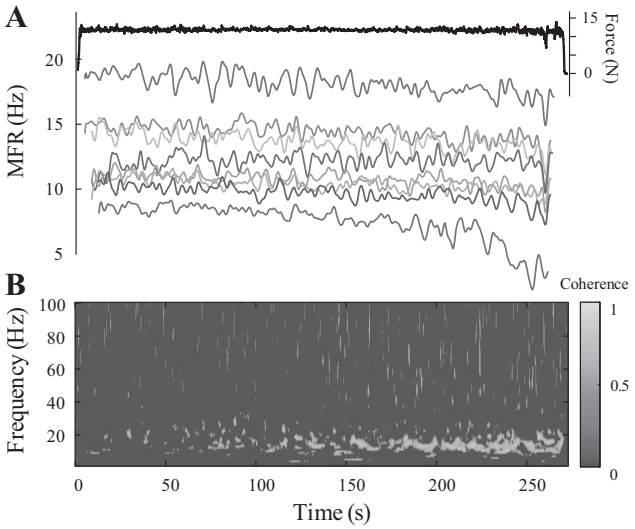

Fig. 6. *A*: force trace and time-varying MFR of 8 MUs (obtained by low-pass filtering the impulse train with a Hanning window of 5-s duration). *B*: median wavelet coherence between composite MU trains over the fatiguing contraction for the same subject as in *A*.

within that band over the fatiguing contraction ($r = -0.7$, $P = 0.019$; $r = -0.55$, $P < 0.01$; and $r = -0.71$, $P = 0.018$, respectively; Fig. 7*A*). However, this correlation was not significant for the gamma band ($r = -0.59$, $P = 0.055$). No significant relationship was observed between the magnitude of the change in MU MFR and the change in beta-band coherence ($r_s = -0.48$, $P = 0.13$) or between the average MU firing rate and the strength of the beta coherence observed ($r_s = 0.4$, $P = 0.2$).

Synchronization was quantified only during the sustained fatiguing contraction, because the pre- and postfatigue trials were not sufficiently long to obtain an accurate estimate. The percentage of MU pairs that displayed significant synchronization was 88.7% and 92.9% in the first and second half of the fatiguing contraction, respectively. In the second half of the contraction, the mean SI of the MUs that displayed significant synchronization increased (from 11 ± 3% to 15 ± 4.6%, $P < 0.001$; Fig. 7*B*). There was a significant correlation between the coefficient of variation of the force and the percent change in coherence within the delta ($r_s = 0.76$, $P < 0.01$; Fig. 7*C*) but not the alpha or beta frequency bands ($r_s = 0.5$, $P = 0.11$ and $r_s = 0.44$, $P = 0.18$, respectively).

Simulation results. Using the model, the effect of common or shared neural inputs to the motoneuron pool, changes in MU MFR, and inhibition of motoneurons were each examined to identify the factors that could contribute to the experimentally observed increase in beta-band coherence. The magnitude of the common component of the input signal to the motoneuron pool was first increased to examine the effect on the beta coherence between MU firings (Fig. 8, *A* and *B*). The integral of the significant coherence in the beta band in the model increased when a common input amplitude of 0.6 mV was applied to the motoneuron pool, and increased further at a common input amplitude of 0.8 mV (Fig. 9*B*).

To examine the effect of MU MFR on the coherence estimate, the median beta-band coherence was examined at three different firing rates, with a shared beta-band input of 0.6 mV (Fig. 8, *C* and *D*). Increasing the MFU of the motoneuron population from 11.3 ± 3 to 12.1 ± 3 Hz resulted in an increase in the median coherence from 6.4 ± 1.4 to 8.6 ± 1.3. A further increase in MFR from 12.1 ± 3 to 13.2 ± 3 Hz increased the median coherence to 8.97 ± 1.5.

Finally, to examine the possible effect of motoneuron inhibition on beta coherence, coherence was estimated after the introduction of inhibition in the presence of a common input of amplitude 0.6 mV (and a resulting reduction in MU MFR from 12.1 ± 3 to 10 ± 3 Hz) and was found to decrease from 8.6 ± 1.5 to 6.9 ± 1.5. When an increase in the magnitude of the common input to the motoneuron pool (0.6 to 0.8 mV) and an inhibition-induced reduction in MU firing rates (12.1 ± 3 to 11 ± 3 Hz) were simultaneously simulated, the median coherence displayed an increase similar to what was observed experimentally (8.6 ± 1.3 to 15 ± 1.4; Fig. 9).

DISCUSSION

Since the appearance of grouped MU activity with muscle fatigue was first reported (Buchthal and Madsen 1950), it has been widely accepted that an increase in the synchronization between the firing times of simultaneously active MUs occurs with the onset of fatigue. However, although estimates of MU synchronization inferred from the surface EMG interference signal support this hypothesis (Beretta-Piccoli et al. 2015; Holtermann et al. 2009; Webber et al. 1995), direct evidence of a fatigue-induced increase in short-term synchronization or beta-range oscillatory coupling between the firing times of simultaneously active MUs within a single muscle has not yet been shown. This study presents direct affirmation of an

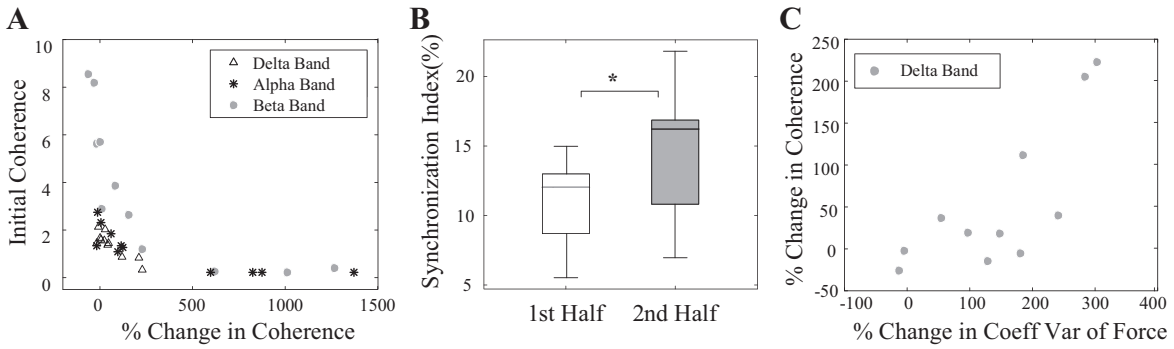

Fig. 7. *A*: relationship between the initial coherence in the alpha and beta bands and the percent change in the integral of the wavelet coherence over the course of the fatiguing contraction. *B*: median and SD of the synchronization index across all subjects for the first and second half of the contraction. * $P < 0.001$. *C*: relationship between the percent change in coherence and the percent change in the coefficient of variation (Coeff Var) of the force.

Downloaded from www.physiology.org/journal/jn at Univ Col Dublin (137.043.113.222) on April 1, 2019.

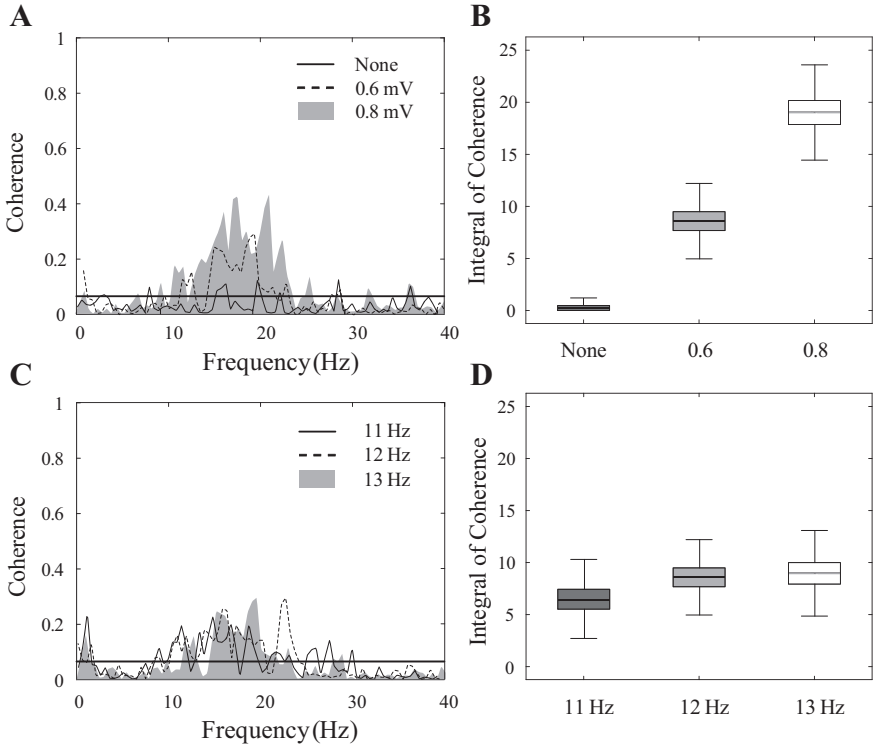

Fig. 8. *A*: MU coherence estimate with no common input to the motoneuron pool (none) or with a beta-band input of magnitude 0.6 or 0.8 mV, with a median MFR of 12.2 ± 3 Hz across the MU pool. *B*: median and SD of the coherence estimates over all pairs of MU composite trains. *C*: MU coherence estimate for varying MU MFR. *D*: median and SD of the coherence estimates over all pairs of MU composite trains, with a beta-band input of magnitude 0.6 mV for the 3 corresponding firing rates.

increase in beta-band MU coherence postfatigue, within MUs of the same muscle, for the first time (Fig. 4*C*). The increased coherence postfatigue was preceded by increases in the beta-band MU coherence and short-term MU synchronization over the course of the fatiguing contraction (Figs. 6*B* and 7). Subjects with high initial beta-band MU coherence showed little change in coherence during the fatiguing contraction, possibly indicating a saturation effect (Fig. 7*A*) whereby no further increase in neural oscillatory activity is possible beyond a certain point. In addition, increases in delta- and alpha-band coherence were observed both during the fatiguing contraction and directly postfatigue. After 10 min of recovery, there was no significant difference between the coherence estimates and those obtained prefatigue for any of the frequency bands.

This study extends the results of previous studies reporting a significant increase in beta-band intermuscular coherence between surface EMG following isometric fatigue (Chang et al. 2012; Danna-Dos Santos et al. 2010; Kattla and Lowery 2010; Wang et al. 2015). However, other studies have reported no significant increase in beta-band EMG-EMG or MU coherence during sustained fatiguing contractions in the elbow flexor muscles (Semmler et al. 2013) and in the tibialis anterior muscle (Castronovo et al. 2015), respectively. Furthermore, although an increase in beta-band corticomuscular coherence has been reported postfatigue in the extensor digitorum communis (Tecchio et al. 2006) and the tibialis anterior (Ushiyama et al. 2011), a weakening of beta coherence has also been reported during sustained (Yang et al. 2009) elbow flexion and in the flexor digitorum profundus, but not flexor digitorum superficialis, following maximal, intermittent handgrip contractions (Yang et al. 2010). These discrepancies highlight that the presence of correlated MU firings in the beta band is likely muscle specific and task dependent, and may relate to the weaker contribution of the corticospinal pathway to proximal compared with distal muscles (Palmer and Ashby 1992). Changes in intramuscular beta coherence may be a more accurate reflection of underlying changes in the synchronous common inputs to the motoneuron pool than corresponding alterations in intermuscular coherence, since the MU spike trains used in the coherence analysis were recorded within the same muscle, at the same force level. This may mitigate some of the uncertainty in the synchronization estimate when com-

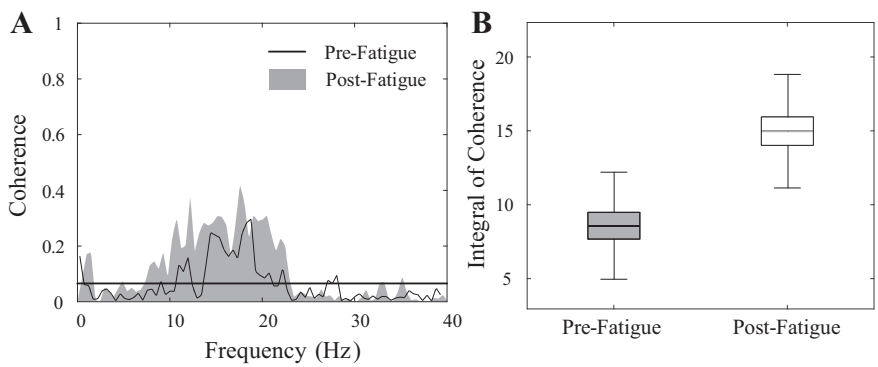

Fig. 9. *A*: coherence spectrum for the pair of MU composite trains with the highest level of coherence, with a beta-band input of magnitude 0.6 mV (prefatigue) or 0.8 mV with inhibition (postfatigue). *B*: median and SD of the coherence estimates over all pairs of MU composite trains.

Downloaded from www.physiology.org/journal/jn at Univ Col Dublin (137.043.113.222) on April 1, 2019.

parisons are made across muscles with different firing characteristics, active at various force levels (Kline and De Luca 2015). Furthermore, MU coherence estimates derived directly from MU spike trains limit sources of variability present in surface EMG coherence that may arise from intersubject differences in subcutaneous tissue and muscle composition.

It remains unclear whether increased beta-band coherence has a functional role or whether it is epiphenomenal in nature, reflecting underlying changes in cortical or other neural firing patterns. It is possible that the increase in beta-band MU coherence and MU short-term synchronization observed in this study may reflect higher attentional demands and a greater amount of motor-related neural processing as fatigue progresses (Schmied et al. 2000). A decrease in the magnitude of oscillatory inputs to the motoneuron pool has been shown to cause more variability in MU firing trains and decrease the number of motoneurons recruited to the contraction (Parkis et al. 2003). Therefore, it is also possible that an increase in synchronized neural inputs may serve to overcome reduced motoneuron excitability and increase recruitment after fatigue (Andersen et al. 2003).

The increase in correlated MU discharges in the delta and alpha frequency bands observed in this study was previously reported following sustained submaximal fatiguing contractions in the tibialis anterior muscle (Castronovo et al. 2015) and in elbow flexor muscles (Semmler et al. 2013). Both synchronization and MU coherence ($<$10 Hz) have been found to increase following muscle damage induced by eccentric exercise (Dartnall et al. 2008). The restoration of low-frequency coherence to prefatigue values after the rest period, however, suggests that muscle damage was not a major factor in the coherence increase directly postfatigue. The increase in coherent MU discharges in the delta-band range observed in the present study was significantly correlated with the coefficient of variation of the force trace (Fig. 7*C*). Contessa et al. (2009) observed an increase in the common drive during fatigue, defined in terms of the cross-correlation between MU firing rates and analogous to MU coherence in the 0-to 4-Hz range (Myers et al. 2004), which was similarly correlated with the force variability. Alpha- and beta-band coherence were not significantly correlated with force variability, which may be expected, because simulation studies have shown that MFR fluctuations in the 1- to 4-Hz range have the greatest relative effect on force variability due to the low-pass filtering effect of the MU twitch response (Lowery and Erim 2005). Delta-band coherence may be influenced by recruitment via feedback from muscle spindles, and possibly the Golgi tendon organs (De Luca et al. 2009). Synchrony in the alpha band is also known to be influenced by the modulation of muscle spindle activity in mechanical and reflex loop resonances (Erimaki and Christakos 2008).

Firing rate. The MFR of the MU population decreased immediately postfatigue and recovered following the 10-min rest period (Fig. 2). In addition, there was a reduction in the firing rates of the majority of MUs (75%) during the sustained fatiguing contraction (Figs. 5 and 6A). This mirrors the results of previous studies that have shown a reduction in MU firing rate during intermittent and constant-force submaximal isometric fatiguing contractions (Duchateau et al. 2002; Garland et al. 1994). Garland et al. (1994) observed changes in the discharge rates of single MUs in the biceps brachii, held just above their threshold of recruitment force. In the present study, changes in discharge rate in a large sample of MUs, concurrently active at the same relative force level, were examined for the first time during a sustained, fatiguing contraction.

Although relatively small, the magnitude of the changes in MU MFR during and postfatigue, were comparable to the modest increase in interpulse interval reported in the biceps brachii (Garland et al. 1994). There is evidence that metabolically and mechanically sensitive group III and IV afferents are in part responsible for the decline in motoneuron discharge rate in fatiguing contractions at maximal force levels (Bigland-Ritchie et al. 1986; Garland and McComas 1990), acting at the spinal and/or the supraspinal level (Gandevia 2001). However, a withdrawal of Ia facilitation from muscle spindles (Macefield et al. 1991) or intrinsic motoneuron properties (Spielmann et al. 1993) could also contribute. The alterations in MU coherence postfatigue and during recovery followed a similar time course to the changes observed in the MU firing rate and action potential duration presented in McManus et al. (2015a). Sensory ascending pathways can modulate the strength of beta-range corticomuscular coupling (McClelland et al. 2012), although the contribution of various afferent groups are not yet clear (Schmied et al. 2014). It is therefore possible that both the magnitude of MU firing rates and the degree of synchronized MU firings could be affected by increased afferent feedback in response to ionic and metabolic changes within the muscle.

Model simulation. The increase in MU coherence immediately postfatigue and during the sustained fatiguing contraction is likely to be multifactorial, but the relative contribution of each factor is not clear. Model simulation was used to investigate how alterations in mean MU firing rate and the introduction of inhibitory feedback to the motoneuron pool can affect the coherence estimate obtained. The simulation studies, however, indicated that neither changes in mean MU firing rate of the magnitude observed experimentally nor simulated inhibition of the motoneuron pool could individually account for the change in coherence observed (Fig. 8, *C* and *D*).

In the model, when the MFR increased toward the median frequency of the common input, an increase in the estimated coherence was observed without any corresponding increase in the amplitude of the shared input (Fig. 8), as previously demonstrated in simulation studies (Lowery et al. 2007). The efficacy of shared oscillatory inputs in eliciting synchronized motoneuron firings increases when the motoneuron firing rates and the frequency of the oscillatory input are similar (Lowery and Erim 2005). In the experimental data, however, the observed reduction in MU MFR is unlikely to have affected the coherence estimate, due to the already low average values (10.8 ± 1.2 Hz). The introduction of inhibition in the model, in the presence of a common correlated input to the motoneuron pool, decreased the coherence estimate by 20%. An increase in the ratio between the independent components of the synaptic input to the motoneuron pool, in this case direct inhibition, and the common correlated inputs may be expected to reduce MU coherence estimates. However, in experimental conditions, the possibility that afferent inputs indirectly enhance the coherence estimate via supraspinal centers cannot be ruled out (Gandevia 2001).

In contrast to the moderate differences in the coherence estimate induced by alterations in MU MFR and the introduction of inhibition, a large increase in the coherence estimate

Downloaded from www.physiology.org/journal/jn at Univ Col Dublin (137.043.113.222) on April 1, 2019.

was observed by raising the amplitude of the common input shared across the motoneuron pool. The magnitude of the change in the coherence spectrum observed experimentally (84%) could be approximated by increasing the amplitude of the shared beta input (74%), while fatigue-induced reductions in MU MFR were replicated with simulated inhibition (Fig. 9).

Study limitations. In this study, decomposition of the surface EMG signal was used to obtain the spike trains representing the firing times of individual MUs within a single muscle. The accuracy of the results depends on the accuracy of the decomposition method. To ensure the reliability of the data, the stability of the MUAP waveform was assessed during the pre- and postfatigue contractions, and during the sustained fatiguing task, to select the most reliable MU firing times for further analysis (Hu et al. 2013). Despite the stringent criteria applied, particularly for the MU trains decomposed from the long fatiguing contraction, there may be inaccuracies in individual firing times present in the spike trains. Frequency-domain MU coherence analysis has been shown to be less sensitive to MU firing rates than traditional synchronization-based measures of time-domain correlation (Lowery et al. 2007), which may make it more robust to the presence of some firing time inaccuracies. In addition, the use of composite spike trains may provide a more aggregate measure of the overall coherence in the MU sample and mitigate the influence of minor sources of error. The strict acceptance criteria applied to the stability of the MU waveform may have rejected an undesirably large number of reliable MUs in this study and introduced a possible sampling bias.

The large intersubject variability associated with coherence estimation is a potential limitation of the coherence analysis. The variability in the coherence estimates obtained for each individual may be due to limitations of coherence as an accurate reflection of shared motoneuronal inputs, intrinsic differences in corticomuscular coupling among individuals, or a combination of both. As previously discussed, the interaction between firing rate and coherence may also skew the coherence estimate in some subjects, for example, when the firing rate of the detected MUs is close to the frequency of the observed coherence. Relatively more synchronous firing instances may also be detected if the MU sample for a subject displays a particularly narrow range of firing rates (Kline and De Luca 2015). Nevertheless, consistent results in terms of the direction of the change in coherence were observed across all frequency bands, with all subjects showing an increase in coherence in the delta-band range postfatigue, and 14 of 15 subjects displaying an increase in the alpha- and beta-band ranges.

Last, to investigate the effect of changing MU firing rates and increasing inhibitory inputs on the MU coherence estimate, a simplified model of the motoneuron pool was used. Because the respective contribution and distribution of these inhibitory and excitatory inputs across the motoneuron pool during fatigue are still unclear, the integrated effect of afferent activity was simplified as a net inhibitory input, nonuniformly distributed over the motoneuron pool. Physiologically, no afferent input reaches motoneurons exclusively by a monosynaptic path, and combined interplay between the many motoneuron inputs is complex (Gandevia 2001). However, these assumptions were made to replicate the simultaneous decrease in motoneuron firing rates and continued MU recruitment observed experimentally. It is possible that other forms of simulated inhibitory circuits could enhance the MU coherence around the beta-band. Certain intrinsic properties of motoneurons, such as persistent inward currents (Heckman et al. 2005), may have been altered postfatigue but were not included in this model.

Conclusion. A significant increase was observed in MU coherence in the delta-, alpha-, and beta-band ranges following a sustained, fatiguing contraction, which recovered following a period of rest. A progressive increase in delta-, alpha-, and beta-band MU coherence was observed over the course of the fatiguing contraction, which was examined using wavelet coherence. The increase in MU coherence and short-term synchronization during fatigue were accompanied by a decline in the MFR of the majority of MUs, with larger reductions in MFR associated with higher initial MU firing rates in some subjects. Simulation results suggest that an increase in inhibitory afferent activity postfatigue, and a resulting or independent reduction in MU MFR, cannot account for the magnitude of the increase in beta-band coherence. The increase is, therefore, more likely to arise from a corresponding increase in the correlated common input to the motoneuron pool. MU MFR and coherence recovered following rest, suggesting the possibility that both are modulated by afferent feedback in response to fatigue-induced changes within the muscle. The ability to infer information about oscillatory cortical and subcortical processes from the peripheral signal gives a novel insight into the adaptations taking place in the central and peripheral nervous system during fatigue.

GRANTS

Funding was provided by the Irish Research Council.

DISCLOSURES

No conflicts of interest, financial or otherwise, are declared by the authors.

AUTHOR CONTRIBUTIONS

L.M.M. and M.M.L. conception and design of research; L.M.M., X.H., and N.L.S. performed experiments; L.M.M. and M.M.L. analyzed data; L.M.M. and M.M.L. interpreted results of experiments; L.M.M. prepared figures; L.M.M. and M.M.L. drafted manuscript; L.M.M., X.H., W.Z.R., N.L.S., and M.M.L. edited and revised manuscript; L.M.M., X.H., W.Z.R., N.L.S., and M.M.L. approved final version of manuscript.

REFERENCES

Andersen B, Westlund B, Krarup C. Failure of activation of spinal motoneurones after muscle fatigue in healthy subjects studied by transcranial magnetic stimulation. *J Physiol* 551: 345–356, 2003.

Beretta-Piccoli M, D'Antona G, Barbero M, Fisher B, Dieli-Conwright CM, Clijsen R, Cescon C. Evaluation of central and peripheral fatigue in the quadriceps using fractal dimension and conduction velocity in young females. *PLoS One* 10: e0123921, 2015.

Bigland-Ritchie B, Furbush F, Woods J. Fatigue of intermittent submaximal voluntary contractions central and peripheral factors. *J Appl Physiol* 61: 421–429, 1986.

Buchthal F, Guld C, Rosenfalck F. Multielectrode study of the territory of a motor unit. *Acta Physiol Scand* 39: 83–104, 1957.

Buchthal F, Madsen A. Synchronous activity in normal and atrophic muscle. *Electroencephalogr Clin Neurophysiol* 2: 425–444, 1950.

Castronovo AM, Negro F, Conforto S, Farina D. The proportion of common synaptic input to motor neurons increases with an increase in net excitatory input. *J Appl Physiol* 119: 1337–1346, 2015.

Chang YJ, Chou CC, Chan HL, Hsu MJ, Yeh MY, Fang CY, Chuang YF, Wei SH, Lien HY. Increases of quadriceps inter-muscular cross-correlation

Downloaded from www.physiology.org/journal/jn at Univ Col Dublin (137.043.113.222) on April 1, 2019.

and coherence during exhausting stepping exercise. *Sensors (Basel)* 12: 16353–16367, 2012.

Contessa P, Adam A, De Luca CJ. Motor unit control and force fluctuation during fatigue. *J Appl Physiol* 107: 235–243, 2009.

Danna-Dos. Santos A, Poston B, Jesunathadas M, Bobich LR, Hamm TM, Santello M. Influence of fatigue on hand muscle coordination and EMG-EMG coherence during three-digit grasping. *J Neurophysiol* 104: 3576–3587, 2010.

Dartnall TJ, Nordstrom MA, Semmler JG. Motor unit synchronization is increased in biceps brachii after exercise-induced damage to elbow flexor muscles. *J Neurophysiol* 99: 1008–1019, 2008.

De Luca CJ, Roy AM, Erim Z. Synchronization of motor-unit firings in several human muscles. *J Neurophysiol* 70: 2010–2023, 1993.

De Luca CJ, Gonzalez-Cueto JA, Bonato P, Adam A. Motor unit recruitment and proprioceptive feedback decrease the common drive. *J Neurophysiol* 101: 1620–1628, 2009.

Duchateau J, Balestra C, Carpentier A, Hainaut K. Reflex regulation during sustained and intermittent submaximal contractions in humans. *J Physiol* 541: 959–967, 2002.

Erimaki S, Christakos CN. Coherent motor unit rhythms in the 6–10 Hz range during time-varying voluntary muscle contractions: neural mechanism and relation to rhythmical motor control. *J Neurophysiol* 99: 473–483, 2008.

Feinstein B, Lindegård B, Nyman E, Wohlfart G. Morphologic studies of motor units in normal human muscles. *Acta Anat (Basel)* 23: 127–142, 1955.

Freund HJ. Motor unit and muscle activity in voluntary motor control. *Physiol Rev* 63: 387–436, 1983.

Gandevia S. Spinal and supraspinal factors in human muscle fatigue. *Physiol Rev* 81: 1725–1789, 2001.

Garland S, Enoka R, Serrano L, Robinson G. Behavior of motor units in human biceps brachii during a submaximal fatiguing contraction. *J Appl Physiol* 76: 2411–2419, 1994.

Garland SJ, McComas A. Reflex inhibition of human soleus muscle during fatigue. *J Physiol* 429: 17–27, 1990.

Hamm TM, Sasaki S, Stuart DG, Windhorst U, Yuan C. The measurement of single motor-axon recurrent inhibitory post-synaptic potentials in the cat. *J Physiol* 388: 631–651, 1987.

Heckman C, Gorassini MA, Bennett DJ. Persistent inward currents in motoneuron dendrites: implications for motor output. *Muscle Nerve* 31: 135–156, 2005.

Holtermann A, Grönlund C, Karlsson JS, Roeleveld K. Motor unit synchronization during fatigue: described with a novel sEMG method based on large motor unit samples. *J Electromyogr Kinesiol* 19: 232–241, 2009.

Hu X, Rymer WZ, Suresh NL. Reliability of spike triggered averaging of the surface electromyogram for motor unit action potential estimation. *Muscle Nerve* 48: 557–570, 2013.

Infantolino BW, Challis JH. Architectural properties of the first dorsal interosseous muscle. *J Anat* 216: 463–469, 2010.

Kattla S, Lowery MM. Fatigue related changes in electromyographic coherence between synergistic hand muscles. *Exp Brain Res* 202: 89–99, 2010.

Kline JC, De Luca CJ. Synchronization of motor unit firings: an epiphenomenon of firing rate characteristics not common inputs. *J Neurophysiol* 115: 178–192, 2015.

Lachaux JP, Lutz A, Rudrauf D, Cosmelli D, Le Van Quyen M, Martinerie J, Varela F. Estimating the time-course of coherence between single-trial brain signals: an introduction to wavelet coherence. *Clin Neurophysiol* 32: 157–174, 2002.

Lowery MM, Erim Z. A simulation study to examine the effect of common motoneuron inputs on correlated patterns of motor unit discharge. *J Comput Neurosci* 19: 107–124, 2005.

Lowery MM, Myers LJ, Erim Z. Coherence between motor unit discharges in response to shared neural inputs. *J Neurosci Methods* 163: 384–391, 2007.

Lowery MM, Vaughan CL, Nolan PJ, O'Malley MJ. Spectral compression of the electromyographic signal due to decreasing muscle fiber conduction velocity. *IEEE Trans Rehabil Eng* 8: 353–361, 2000.

Macefield G, Hagbarth KE, Gorman R, Gandevia S, Burke D. Decline in spindle support to alpha-motoneurones during sustained voluntary contractions. *J Physiol* 440: 497–512, 1991.

McClelland VM, Cvetkovic Z, Mills KR. Modulation of corticomuscular coherence by peripheral stimuli. *Exp Brain Res* 219: 275–292, 2012.

McManus L, Hu X, Rymer WZ, Lowery MM, Suresh NL. Changes in motor unit behavior following isometric fatigue of the first dorsal interosseous muscle. *J Neurophysiol* 113: 3186–3196, 2015a.

McManus LM, Hu X, Rymer WZ, Suresh NL, Lowery MM. Fatigue-related alterations to intra-muscular coherence. *2015 7th International IEEE/EMBS Conference on Neural Engineering (NER)*, Montpellier, France, April 22–25, 2015, p. 902–905.

Myers LJ, Erim Z, Lowery MM. Time and frequency domain methods for quantifying common modulation of motor unit firing patterns. *J Neuroeng Rehabil* 1: 2, 2004.

Nawab SH, Chang SS, De Luca CJ. High-yield decomposition of surface EMG signals. *Clin Neurophysiol* 121: 1602–1615, 2010.

Nordstrom MA, Miles TS, Türker K. Synchronization of motor units in human masseter during a prolonged isometric contraction. *J Physiol* 426: 409–421, 1990.

Palmer E, Ashby P. Corticospinal projections to upper limb motoneurones in humans. *J Physiol* 448: 397–412, 1992.

Parkis MA, Feldman JL, Robinson DM, Funk GD. Oscillations in endogenous inputs to neurons affect excitability and signal processing. *J Neurosci* 23: 8152–8158, 2003.

Powers RK. A variable-threshold motoneuron model that incorporates time- and voltage-dependent potassium and calcium conductances. *J Neurophysiol* 70: 246–262, 1993.

Schmied A, Forget R, Vedel JP. Motor unit firing pattern, synchrony and coherence in a deafferented patient. *Front Hum Neurosci* 8: 2014.

Schmied A, Pagni S, Sturm H, Vedel JP. Selective enhancement of motoneurone short-term synchrony during an attention-demanding task. *Exp Brain Res* 133: 377–390, 2000.

Semmler JG, Ebert SA, Amarasena J. Eccentric muscle damage increases intermuscular coherence during a fatiguing isometric contraction. *Acta Physiol (Oxf)* 208: 362–375, 2013.

Spielmann J, Laouris Y, Nordstrom M, Robinson G, Reinking R, Stuart D. Adaptation of cat motoneurons to sustained and intermittent extracellular activation. *J Physiol* 464: 75–120, 1993.

Talebinejad M, Chan AD, Miri A. Fatigue estimation using a novel multifractal detrended fluctuation analysis-based approach. *J Electromyogr Kinesiol* 20: 433–439, 2010.

Tecchio F, Porcaro C, Zappasodi F, Pesenti A, Ercolani M, Rossini PM. Cortical short-term fatigue effects assessed via rhythmic brain-muscle coherence. *Exp Brain Res* 174: 144–151, 2006.

Terry K, Griffin L. How computational technique and spike train properties affect coherence detection. *J Neurosci Methods* 168: 212–223, 2008.

Ushiyama J, Katsu M, Masakado Y, Kimura A, Liu M, Ushiba J. Muscle fatigue-induced enhancement of corticomuscular coherence following sustained submaximal isometric contraction of the tibialis anterior muscle. *J Appl Physiol* 110: 1233–1240, 2011.

Wang L, Lu A, Zhang S, Niu W, Zheng F, Gong M. Fatigue-related electromyographic coherence and phase synchronization analysis between antagonistic elbow muscles. *Exp Brain Res* 233: 971–982, 2015.

Webber C, Schmidt M, Walsh J. Influence of isometric loading on biceps EMG dynamics as assessed by linear and nonlinear tools. *J Appl Physiol* 78: 814–822, 1995.

Yang Q, Fang Y, Sun CK, Siemionow V, Ranganathan VK, Khoshknabi D, Davis MP, Walsh D, Sahgal V, Yue GH. Weakening of functional corticomuscular coupling during muscle fatigue. *Brain Res* 1250: 101–112, 2009.

Yang Q, Siemionow V, Yao W, Sahgal V, Yue GH. Single-trial EEG-EMG coherence analysis reveals muscle fatigue-related progressive alterations in corticomuscular coupling. *IEEE Trans Neural Syst Rehabil Eng* 18: 97–106, 2010.

Downloaded from www.physiology.org/journal/jn at Univ Col Dublin (137.043.113.222) on April 1, 2019.